

# Catalysis Science & Technology

Accepted Manuscript



This is an *Accepted Manuscript*, which has been through the Royal Society of Chemistry peer review process and has been accepted for publication.

*Accepted Manuscripts* are published online shortly after acceptance, before technical editing, formatting and proof reading. Using this free service, authors can make their results available to the community, in citable form, before we publish the edited article. We will replace this *Accepted Manuscript* with the edited and formatted *Advance Article* as soon as it is available.

You can find more information about *Accepted Manuscripts* in the [Information for Authors](#).

Please note that technical editing may introduce minor changes to the text and/or graphics, which may alter content. The journal's standard [Terms & Conditions](#) and the [Ethical guidelines](#) still apply. In no event shall the Royal Society of Chemistry be held responsible for any errors or omissions in this *Accepted Manuscript* or any consequences arising from the use of any information it contains.

# Mechanistic insights into hydrogen generation for catalytic hydrolysis and alcoholysis of silanes with high-valent oxorhenium(V) Complexes

Cite this: DOI: 10.1039/x0xx00000x

Received 00th January 2012,  
Accepted 00th January 2012

DOI: 10.1039/x0xx00000x

www.rsc.org/

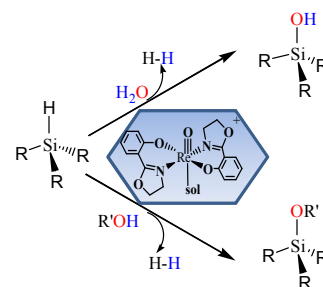
Wenmin Wang, Jiandi Wang, Liangfang Huang, and Haiyan Wei\*

The high-valent oxorhenium(V) complex  $[\text{Re}(\text{O})(\text{hoz})_2]^+$  (**1**)-catalyzed the hydrolytic oxidation of silanes to produce dihydrogen was studied computationally to determine the underlying mechanism. Our results suggested that the oxorhenium(V) complex **1**-catalyzed the hydrolysis/alcoholysis of silanes proceeds via the ionic out-sphere mechanistic pathway. The turnover-limiting step was found to be heterolytic cleavage of the Si–H bond and featured a  $\text{S}_{\text{N}}2\text{-Si}$  transition state, which corresponds to nucleophilic *anti* attack of water or alcohol on the silicon atom in a *cis*  $\eta^1$ -silane rhenium(V) adduct. Dihydrogen was generated upon transferring the hydride from the neutral rhenium hydride  $[\text{Re}(\text{O})(\text{hoz})_2\text{H}]$  to the solvated  $[\text{Me}_3\text{SiOHR}]^+$  ion. The activation free energy of the turnover-limiting step along the ionic outer-sphere pathway was calculated at 15.7 kcal/mol with water, 15.4 kcal/mol with methanol, and 15.9 kcal/mol with ethanol. These values are energetically more favorable than the [2+2] addition pathway by  $\sim 15.0$  kcal/mol. Furthermore, the previously proposed catalytic pathways involving transient rhenium(VII) complexes or via the silicon attacking on a rhenium hydroxo/alkoxo complex are shown to possess higher barriers.

## Introduction

Silanols have received considerable attention across industrial fields for their role as building blocks in silicon-based polymeric materials as well as in organic synthesis.<sup>1–5</sup> An attractive synthetic route for silanols is the addition of hydrosilanes to water since the only side-product is hydrogen gas.<sup>6–10</sup> Furthermore, due to the relatively weak of Si–H bond strength,<sup>11–13</sup> the catalytic hydrolysis of Si–H bonds is a promising method for the generation of dihydrogen. In this regard, it is highly desirable to find effective chemical methods for achieving efficient hydrogen production from water.<sup>14–16</sup> As such, a series of heterogeneous catalysts based on metal nanoparticles (Pd/AlO(OH),<sup>17</sup> Pd/Al<sub>2</sub>O<sub>3</sub>,<sup>18</sup> AuCNT,<sup>19</sup> RuHAP<sup>20</sup>, etc<sup>21</sup>) and homogeneous transition metal catalysts, such as gold,<sup>22</sup> rhodium,<sup>23</sup> iridium,<sup>24</sup> rhenium,<sup>15</sup> ruthenium,<sup>25</sup> nickel,<sup>26</sup> cobalt,<sup>27</sup> iron,<sup>28</sup> or molybdenum<sup>29,30</sup>, have been reported to show excellent activities for the production of dihydrogen from hydrosilanes and water. Very recently, Abu-Omar *et al.* described an air- and water-stable oxorhenium(V) complex  $[\text{Re}(\text{O})(\text{hoz})_2]^+$  (hoz = 2-(2'-hydroxyphenyl)-2-oxazoline(-) (**1**) (Scheme 1) that catalyzes the hydrolytic oxidation of organosilanes to produce dihydrogen under ambient conditions, resulting in quantitative hydrogen yields. In addition, this process required low catalyst loading and no solvent.<sup>15,31</sup>

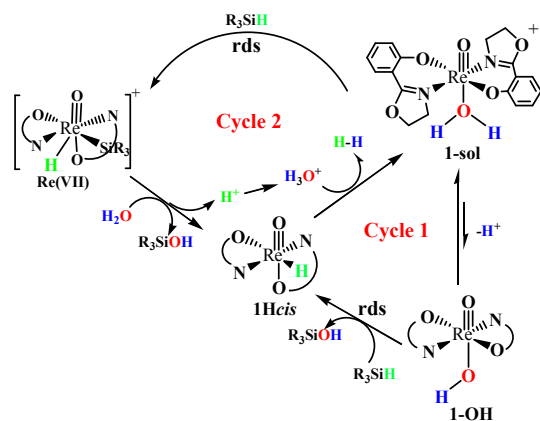
**Scheme 1** The catalytic hydrolysis and alcoholysis of silanes by the high-valent oxorhenium(V) complex  $[\text{Re}(\text{O})(\text{hoz})_2]^+$  (hoz = 2-(2'-hydroxyphenyl)-2-oxazoline(-) (**1**).



The catalytic reaction depicted in Scheme 1 presents a new methodology for the production of hydrogen from organic liquid using only water as a co-reagent. Specifically, this was the first example of employing a high-valent oxo-metal complex for the dehydrogenative oxidation of hydrosilanes using water and alcohols. Based on kinetic data and isotope labeling experiments, Abu-Omar *et al.* have proposed two possible pathways for this reaction (Scheme 2).<sup>31</sup> **Cycle 1** begins with an attack of the silicon atom in silane onto a hydroxo/alkoxo ligand bonding at the rhenium center in a

rhenium hydroxo complex (**1-OH**). This process results in a hydride transfer to afford silanol and generating an oxorhenium(V) hydride. The oxorhenium(V) hydride then reacts with the solvated  $[H^+]$  to produce  $H_2$  and regenerates the cationic oxorhenium(V) complex **1**. **Cycle 2** is the traditional oxidative addition mechanism,<sup>32</sup> which involves the formation of a transient rhenium(VII) silyl hydride intermediate via the oxidative addition of Si–H bond to the rhenium(V) center. Water or alcohol then attacks the electrophilic silicon atom to yield silanol. **Cycle 2** is completed via reaction of the oxorhenium(V) hydride with  $H^+$  to produce  $H_2$ .

**Scheme 2** Proposed mechanism for the high-valent oxorhenium(V) complex  $[Re(O)(hoz)_2]^+$  ( $hoz = 2-(2'-hydroxyphenyl)-2-oxazoline(-)$ ) (**1**)-catalyzed the hydrolysis of organosilanes in the literature.<sup>31</sup>



It is clear in both of the proposed catalytic cycles (cycle **1** and cycle **2**), that the generating  $H_2$  gas is comprised of one H atom from silane and one from water. Also, the rates of two proposed catalytic pathways depend on the silane and catalyst concentrations, which is consistent with the observed kinetic experiments demonstrating the involvement of Si–H bonds. Furthermore, it is worth noting that the [3+2] or [2+2] manner of Si–H bond addition across meta-oxo bonds as in other metal oxo systems, such as  $ReO_2(I)(PPh_3)_2$ <sup>33,34</sup>,  $MoO_2Cl_2$ <sup>35,36</sup>, and  $OsO_4$ <sup>37</sup>, is excluded, as Si–H insertion into the  $Re\equiv O$  bond in oxorhenium(V) complex **1** was not detected by Abu-Omar *et al.* However, the exact nature of the active catalytic species is still uncertain. In particular, detailed mechanistic studies on the high-valent oxorhenium(V) catalyst (**1**)-mediated hydrolysis and alcoholysis of silanes have yet to be explored theoretically. In order to obtain a clear understanding of the high-valent oxorhenium(V) catalyst (**1**)-catalyzed hydrolysis and alcoholysis reactions, we have performed theoretical calculations to investigate the plausible reaction pathways using density functional theory.<sup>38</sup> Remarkably, our results show that  $[Re(O)(hoz)_2]^+$  (**1**) mediated the hydrolysis and alcoholysis proceed through an ionic outer-sphere mechanistic pathway. And this preferable catalytic cycle does not involve a hydroxo/alkoxo complex (as in Cycle **1**) or a transient rhenium(VII) complex (as in Cycle **2**).

A variety of recent studies have reported the invocation of the ionic outer-sphere mechanistic pathways.<sup>39</sup> These works include those on the catalytic reduction of carbonyl compounds

using tris(pentafluorophenyl)borane/silanes systems by Piers,<sup>40</sup> the reductions of aldehyde/ketone, epoxides, amides, and ester, alkyl halides by a cationic iridium catalyst/silanes system.<sup>41</sup> However, very few theoretical studies and models on reactions that favor ionic mechanistic pathways mediated by transition metal catalysts have been performed.<sup>42</sup> The calculations presented from this work that illustrates the mechanism for high-valent oxorhenium(V) complex  $[Re(O)(hoz)_2]^+$  (**1**) mediated hydrolysis and alcoholysis of organosilanes to produce  $H_2$  may also be considered to model the reduction reaction of a series of high-valent transition metal catalysts.<sup>43</sup> The knowledge and insight gained from this study can enable future works that may ultimately lead to the design of more efficient catalysts that favor ionic outer-sphere mechanisms.

## Computational Methods

All molecular geometries of the model complexes were optimized at the DFT Becke3LYP (B3LYP) level,<sup>44</sup> which was implemented in Gaussian 09.<sup>45</sup> The effective core potentials (ECPs) of Hay and Wadt with double- $\zeta$  valence basis sets (LanL2DZ)<sup>46</sup> were used to describe the Re metals. In addition, polarization functions were added for Re ( $\zeta_r = 0.869$ ).<sup>47</sup> The 6-311g(d,p) basis set was used for all other atoms, such as C, H, O, N and Cl. All geometric optimizations were performed under solvent conditions using the SMD solvation model with  $CH_2Cl_2$  as the solvent using tight convergence criteria (The SMD model is an IEFPCM calculation with radii and non-electrostatic terms for Truhlar and coworkers' SMD solvation model<sup>48</sup>). Frequency calculations at the same level of theory were carried out to verify all stationary points as minima (zero imaginary frequency) and transition states (one imaginary frequency). The transition states found were further confirmed by calculating intrinsic reaction coordinates routes toward the corresponding minima and reoptimizing from the final phase of IRC paths to reach each minimum. The final Gibbs energy values for  $\Delta G_{sol}$  reported in the current study were relative Gibbs free energies calculated at 298 K in solvent, with corrections for dispersion effects using Grimme's empirical dispersion correction term: i.e., B3LYP-D3.<sup>49</sup> Detailed comparisons of different methods are listed in Supporting Information. All the geometries are displayed using the software of CYLview.<sup>50</sup>

In the calculations, the catalyst  $[Re(O)(hoz)_2]^+$  (the benzene ring on the 2'-hydroxyphenyl is reduced) (**1**), and the trimethylsilane ( $HSiMe_3$ ), water was adopted to study all the possible catalytic steps. Moreover, the key intermediates and transition states for a series of silanes ( $Et_3SiH$ ,  $Et_2MeSiH$ ,  $tBuMeSiH$ ,  $Ph_2MeSiH$ ,  $PhMe_2SiH$  and  $Ph_3SiH$ ) and a series of alcohols ( $CH_3OH$ ,  $CH_3CH_2OH$ ,  $PhOH$ ) were also investigated. For compounds that have multiple conformations, several different starting geometries were set to optimize the structures and compared to locate the lowest-energy conformation.

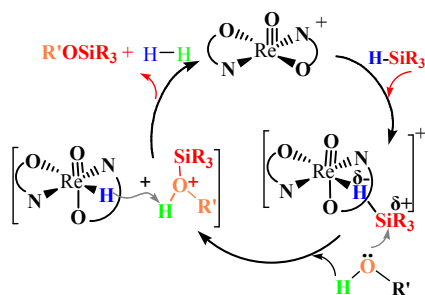
## Results and Discussion

In the subsequent sections, three different reaction possibilities for the cationic high-valent oxorhenium(V)

complex  $[\text{Re}(\text{O})(\text{hoz})_2]^+$  (1)-catalyzed hydrolysis and alcoholysis of silanes are presented and discussed in detail. The first pathway is the ionic outer-sphere pathway, in which nucleophilic organic substrates (water or alcohols) attack the silicon atom in the silane-metal adduct to activate the Si–H bond. The second mechanism, proposed by Abu-Omar *et al.*,<sup>31</sup> (Cycle 1, Scheme 2) involves the attack of Si of silane onto a rhenium hydroxo complex (1-OH). And the third mechanism, (Cycle 2, Scheme 2) involves the oxidative addition of the Si–H bond to the rhenium center to generate a transient rhenium(VII) hydride intermediate.

**Pathway I: Oxorhenium(V) complex (1)-catalyzed hydrolysis/alcoholysis of silanes via the ionic mechanistic pathway.** According to experimental observations,<sup>42,51</sup> the ionic outer-sphere mechanistic pathway can be described as an initial coordination of silane to the metal center of a catalyst, followed by a nucleophilic attack (via water or alcohols) on the silane metal adduct, as shown in Scheme 3. This attack prompts the transfer of the silyl ion ( $\text{R}_3\text{Si}^+$ ) to the water or alcohol and in turn the silane hydride to the metal center. The catalytic cycle is completed by the solvated silyl water/alcohol ion reacting with the metal hydride intermediate, which leads to the final product and the regeneration of the catalyst. Along the ionic outer-sphere pathway, the requirement for coordination of the unsaturated substrates to the metal center is removed.

**Scheme 3** Proposed ionic outer-sphere mechanistic pathway for the high-valent oxorhenium(V) complex  $[\text{Re}(\text{O})(\text{hoz})_2]^+$  (1)-catalyzed the hydrolysis of organosilanes in the current study.



**First Step: Formation of the silane-rhenium complex.** The first step of the ionic outer-sphere pathway is the coordination of a free silane to the rhenium center. The two-electron three-center Si–H–M interaction has been proposed in several compounds. In addition, the relationship of this interaction to Si–H bond activation has been reported.<sup>51a,52</sup> In this work, we demonstrate that a free silane molecule can easily coordinate to the vacant position on rhenium center, yielding  $[\text{Re}(\text{O})(\text{hoz})_2](\text{HSiMe}_3)^+$ , **2trans**. In **2trans** (Figure 1), the silane resides on the axial position of the octahedral structure, *trans* to the multiply bonded oxo ligand. The  $\text{Re}\cdots\text{H}$  distance is significantly long, at 2.75 Å. The  $\text{Re}-\text{H}-\text{Si}$  angle is  $174.7^\circ$  and the Si–H (1.51 Å) distance is slightly longer than that of the free silane molecule (1.49 Å). These results show that the coordination of silane in **2trans** is a much weaker end-on  $\eta^1\text{-H}(\text{Si})$  mode.<sup>53</sup> *Trans* addition of silane to the rhenium center in **1** results in a destabilization energy of 3.5 kcal/mol in the solvent.

The silane rhenium complex could also exist as **2cis** isomer, which describes the silane molecule being  $\eta^1$  bound to the rhenium center, at the equatorial plane of the octahedral structure, lying *cis* to the multiply bonded oxo ligand, shown in Figure 1. In this conformation, the oxazoline oxygen atom occupies the axial position, lying *trans* to the multiply bonded oxo ligand.<sup>54</sup> In **2cis**, the  $\text{Re}\cdots\text{H}$  distance is significantly shorter at only 1.91 Å. The Si–H bond distance (1.57 Å) is 0.08 Å longer than that of a free silane molecule (1.49 Å). And the  $\text{Re}-\text{H}-\text{Si}$  angle is  $152.2^\circ$ . These results show that the coordination of silane in **2cis** is also in a weak, end-on  $\eta^1\text{-H}(\text{Si})$  mode. However, the silane hydrogen lies relatively close to the metal center (1.91 Å) in **2cis**, which is  $\sim 0.84$  Å shorter than in **2trans** (2.75 Å). These parameters indicate that a relative strong coordination between the rhenium center and the silane exist in *cis* conformation. It can be rationalized that the weaker interaction in **2trans** isomer is due to the strong *trans* influence imposed by the multiply bonded oxo ligand.<sup>55</sup>

The isomerization is endergonic where **2cis** is 6.5 kcal/mol less stable than **2trans**. In addition, the transition state corresponding to silane *cis* addition to the rhenium center is calculated to require an activation free energy of 13.2 kcal/mol above **1** and free silane (TS2, Supporting Information).

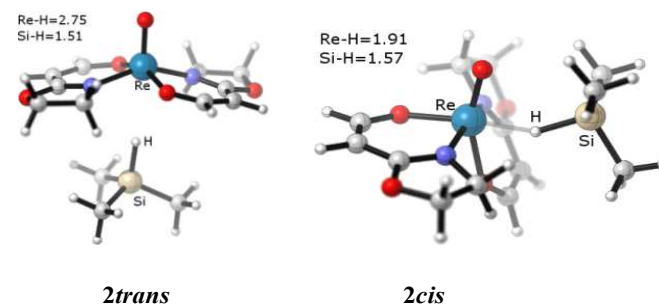


**Figure 1.** Optimized structures of the  $\eta^1$ -silane rhenium complexes: **2trans**, **2cis**.

**Second Step: The cleavage of Si–H bond.** The  $\eta^1$ -silane bound to the electrophilic rhenium(V) center in **2trans** or **2cis** would be activated toward the nucleophilic attack by water. It is worth noting that  $\text{H}_2\text{O}$  molecule can approach the silicon in a “backside” or “frontside” fashion, representing either a  $\text{H}_2\text{O}$  molecule *anti* attacking the silane at the face opposite to the metal center, or a  $\text{H}_2\text{O}$  molecule *syn* attacking the silane at the face same as the metal center. Both isomers were taken as our starting point toward  $\text{H}_2\text{O}$  molecule attacking. In total, four types of conformations were taken into consideration.

First, a  $\text{H}_2\text{O}$  molecule nucleophilically attacks the silicon center in **2trans** in a “backside” fashion. Initially, a loosely bound adduct, **2trans** +  $\text{H}_2\text{O}$ , is formed (Supporting Information). In this adduct, the geometries of **2trans** and  $\text{H}_2\text{O}$  are barely perturbed from their isolated structures ( $d(\text{Si}\cdots\text{O}(\text{H}_2\text{O})) = 4.22$  Å). Using  $\text{H}\cdots\text{Si}$  or  $\text{Si}\cdots\text{O}(\text{H}_2\text{O})$  separation as the reaction coordinates, the search for a transition state in this arrangement has been unsuccessful. The energy plot versus  $d(\text{H}\cdots\text{Si})$  or  $d(\text{Si}\cdots\text{O}(\text{H}_2\text{O}))$  went uphill until it was possible to obtain the neutral rhenium hydride species

(**1Htrans**) and the solvated  $[\text{Me}_3\text{SiOH}_2]^+$  ion. On the free energy surface, the reaction ( $\mathbf{1} + \text{HSiMe}_3 + \text{H}_2\text{O} \rightarrow \mathbf{1Htrans} + \text{Me}_3\text{SiOH}_2^+$ ) is endergonic,  $\Delta G = 29.2$  kcal/mol. Thus, the estimated activation barrier of 29.2 kcal/mol is obtained for  $\text{H}_2\text{O}$  molecule *anti* attacking the  $\eta^1$ -silane rhenium complex **2trans**.

Alternatively, a  $\text{H}_2\text{O}$  molecule could “frontside” attack **2trans**, featuring a  $\text{H}_2\text{O}$  molecule *syn* attacking silane at the same face as the metal center. For such an arrangement, the transition state (**TS3syn**) is located. In the optimized structure of **TS3syn** (Figure 2), the silane hydrogen bond is stretched to 1.74 Å and moves close to the rhenium center at a  $\text{Re}\cdots\text{H}$  distance of 2.00 Å.  $\text{H}_2\text{O}$  molecule coordinates to the silicon center with  $\text{Si}\cdots\text{O}(\text{H}_2\text{O})$  distance of 2.02 Å. The coordination geometry around the silicon center is penta-coordinated and can be regarded as a trigonal bipyramid. The calculated vibrational motion of the imaginary frequency associated with **TS3syn** represents the expected normal mode of a *syn*  $\text{S}_{\text{N}}2$ -Si reaction, with three atoms of  $\text{Re}\cdots\text{H}\cdots\text{Si}$  approximately in a straight line at  $178.5^\circ$  and three atoms of  $\text{H}\cdots\text{Si}\cdots\text{O}(\text{H}_2\text{O})$  roughly perpendicular at  $71.6^\circ$ . These features indicate the nucleophilic attacks by  $\text{H}_2\text{O}$  at the silicon center and simultaneously the electrophilic hydride moiety leaves the silicon center, which results in the cleavage of  $\text{Si}\text{--}\text{H}$  bond and the formation of a  $\text{Re}\text{--}\text{H}$  bond. However, our calculation showed that **TS3syn** is associated with a pronouncedly high activation free energy barrier, 34.4 kcal/mol.

Likewise, a  $\text{H}_2\text{O}$  molecule could nucleophilically approach the silicon center in **2cis** form “frontside” or “backside” to prompt cleavage of the  $\text{Si}\text{--}\text{H}$  bond. The ionic transition states in which  $\text{H}_2\text{O}$  molecules *anti* attack the silicon center at the opposite face to the metal center (**TS4anti**, “backside”) and *syn* attack the silicon center at the same face as the metal center (**TS4syn**, “frontside”) were both located (Figure 2). In **TS4anti**, the coordination geometry around the silicon center is penta-coordinated trigonal bipyramid, where with the silyl group ( $\text{SiMe}_3$ ) acts as the plane and the leaving hydrogen atom and the incoming  $\text{O}(\text{H}_2\text{O})$  atoms occupy the apical positions. The

four atoms of  $\text{Re}\cdots\text{H}\cdots\text{Si}\cdots\text{O}$  are roughly in a straight line, with  $\text{Re}\text{--}\text{H}\text{--}\text{Si}$  having an angle of  $165.5^\circ$  and  $\text{H}\text{--}\text{Si}\text{--}\text{O}$  having an angle of  $173.6^\circ$ . The calculated vibrational motion of the imaginary frequency associated with **TS4anti** represents the expected normal mode of a traditional  $\text{S}_{\text{N}}2$ -Si reaction at the silicon center, which features attack of nucleophilic  $\text{H}_2\text{O}$  group on the silicon center,  $d(\text{Si}\cdots\text{O}) = 2.00$  Å and the electrophilic hydride moiety leaves the silicon center, to prompt the cleavage of the  $\text{Si}\text{--}\text{H}$  bond,  $d(\text{Si}\cdots\text{H}) = 2.05$  Å and the formation of  $\text{Re}\text{--}\text{H}$  bond,  $d(\text{Re}\cdots\text{H}) = 1.70$  Å. Likewise, the transition state **TS4syn** represents the expected normal mode of a *syn*  $\text{S}_{\text{N}}2$ -Si reaction, which features the simultaneous cleavage of the  $\text{Si}\text{--}\text{H}$  bond,  $d(\text{Si}\cdots\text{H}) = 1.91$  Å and the formation of the  $\text{Re}\text{--}\text{H}$  bond,  $d(\text{Re}\cdots\text{H}) = 1.76$  Å, upon the attack of nucleophilic  $\text{H}_2\text{O}$  on the silicon center,  $d(\text{Si}\cdots\text{O}) = 2.08$  Å. The calculated free energy profile shows that *cis*  $\eta^1$ -silane rhenium(V) adduct **2cis** entails a significantly reduction of activation barrier in  $\text{S}_{\text{N}}2$ -Si transition state compared to *trans* isomer. The activation free energy of **TS4anti** is calculated to be much lower at 15.7 kcal/mol. The calculated free energy associated with **TS4syn** is pronouncedly high, at 31.8 kcal/mol. Therefore, both of *syn* arrangements (**TS3syn** and **TS4syn**) can be eliminated as potential mechanisms.

**Third Step: The hydride transfer.** Following **TS4anti**, the reaction goes from two molecular units, **2cis** and a  $\text{H}_2\text{O}$  molecule, to an intermediate **4anti**. In the optimized structure of **4anti** (Figure 3), consisting of the  $[\text{Me}_3\text{SiOH}_2]^+$  ion paired with a *cis* neutral rhenium hydride  $[\text{Re}(\text{O})(\text{hoz})_2\text{H}]$  (**1Hcis**), the rhenium-hydride bond is completely formed,  $d(\text{Re}\text{--}\text{H}) = 1.65$  Å, the  $\text{Si}\text{--}\text{H}$  bond is completely cleaved and largely separated (3.98 Å). **4anti** was calculated to be 6.7 kcal/mol below **TS4anti** using B3LYP calculations. However, when dispersion effects were considered at the B3LYP-D level, the free energy of **4anti** was 1.5 kcal/mol higher than **TS4anti**.<sup>56</sup>

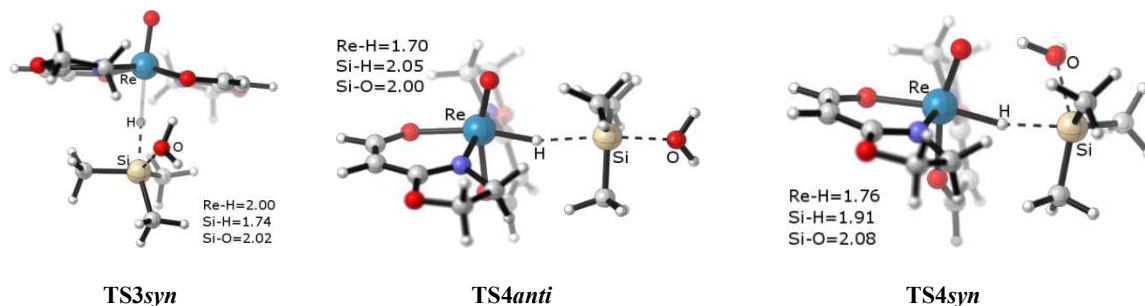


**Figure 2.** Optimized structures of the ionic transition state, **TS3syn** representing  $\text{H}_2\text{O}$  molecule *syn* attacking the silane center in **2trans**, and the ionic transition states, **TS4anti** and **TS4syn** representing  $\text{H}_2\text{O}$  molecule *anti* and *syn* attacking the silane center in **2cis**, respectively. Bond distances are shown in Å.

## ARTICLE

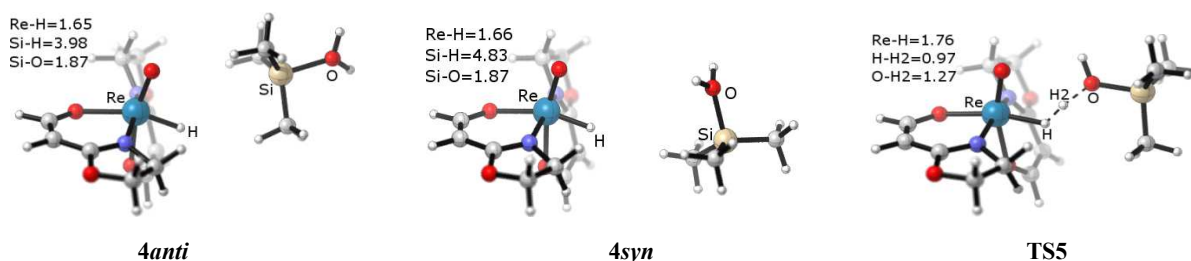


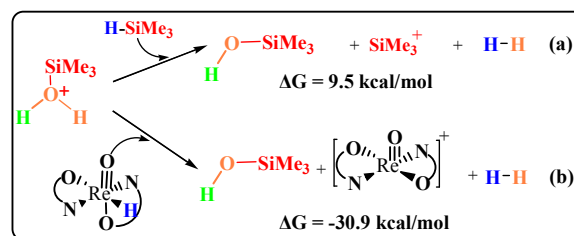
**Figure 3.** Optimized structures of the intermediates **4anti**, **4syn** comprised of the  $[\text{Me}_3\text{SiOH}_2]^+$  ion and the neutral rhenium hydride  $[\text{Re}(\text{O})(\text{hoz})_2(\text{H})]$ , and the transition state **TS5** representing  $[\text{Me}_3\text{SiOH}_2]^+$  ion abstracting the hydride at the neutral rhenium hydride  $[\text{Re}(\text{O})(\text{hoz})_2(\text{H})]$  to produce  $\text{H}_2$  and silanol. Bond distances are shown in Å.

The catalytic cycle is then completed when the protonated silyl ion abstract a hydrogen to produce dihydrogen and generate silanol. Initially, **4anti** could dissociate to yield the neutral rhenium hydride  $[\text{Re}(\text{O})(\text{hoz})_2\text{H}]$  (**1Hcis**) and the silyl water ion  $[\text{Me}_3\text{SiOH}_2]^+$ , which lies 5.0 kcal/mol lower than that of **4anti**. At this point, two diverging routes were evaluated. The first route considers that two species rearrange to form another isomer, **4syn** (Figure 3). In other words,  $\text{H}_2\text{O}$  molecule is located around the silicon atom center at the face same as the metal center in **4syn**, compared to the *anti* parallel arrangement in **4anti**. The geometries of two species of rhenium hydride **1Hcis** and the solvated  $[\text{Me}_3\text{SiOH}_2]^+$  ion in **4syn** show negligible changes. This isomerization yields a stabilization energy of 3.4 kcal/mol. Next, the  $[\text{Me}_3\text{SiOH}_2]^+$  ion abstract a hydride at the rhenium hydride to produce dihydrogen and regenerate the catalyst. This process readily occurs by passing the transition state **TS5** (Figure 3). In **TS5**, the hydride on the rhenium center moves to the O–H2 bond, with distance of  $d(\text{H}\cdots\text{H}_2) = 0.97$  Å. And the hydrogen atom (H2) leaves the  $[\text{Me}_3\text{SiOH}_2]^+$  ion with a distance of  $d(\text{O}\cdots\text{H}_2) = 1.27$  Å. The eigenvector associated with **TS5** involves approach of the hydride bound at the rhenium center to the hydrogen atom of O–H2 bond at the  $[\text{SiMe}_3\text{OH}_2]^+$  ion. IRC calculations were carried out from the transition state **TS5** leading to the formation of dihydrogen gas and silanol product. **TS5** is calculated at 0.2 kcal/mol higher than that of **4syn** intermediate at the B3LYP calculated level. However, when dispersion effects were considered at the B3LYP-D level, the free energy of **TS5** was 5.1 kcal/mol lower than **4syn**.<sup>57</sup>

Also, there is the possibility for the  $[\text{Me}_3\text{SiOH}_2]^+$  ion abstracting a hydride from free silanes (Scheme 4, (a)), however, this reaction is calculated to be endoergic, with  $\Delta G = 9.5$  kcal/mol. Therefore, despite being the most available hydride source, due to the endoergic nature of the reaction, it is unlikely that free silanes function as hydride donors in this catalytic process. Furthermore, the overall reaction for the rhenium hydride *cis*- $\text{Re}(\text{O})(\text{hoz})_2\text{H}$  (**1Hcis**) donating a hydride

to the  $[\text{Me}_3\text{SiOH}_2]^+$  ion is largely exergonic (Scheme 4, (b)),  $\Delta G = -30.9$  kcal/mol. Therefore, we conclude that the hydride transfer process from rhenium hydride **1Hcis** to the  $[\text{Me}_3\text{SiOH}_2]^+$  ion is a kinetically and thermodynamically favored reaction. Clearly, the ion pairs comprised of a neutral rhenium hydride species and the solvated  $[\text{Me}_3\text{SiOH}_2]^+$  ion are metastable which undergo easy isomerization to produce  $\text{H}_2$  and yield silanol. The significant accumulation of neutral rhenium hydride species is unlikely under these reaction conditions. Furthermore, our calculated results suggest that the catalytic cycle is more likely to proceed without the generation of a free rhenium hydride species or  $[\text{Me}_3\text{SiOH}_2]^+$  ion.

**Scheme 4** The reactions for the  $[\text{Me}_3\text{SiOH}_2]^+$  ion abstracting a hydride from free silanes (a), or from the rhenium hydride **1Hcis** (b).



In summary, the calculated free-energy profiles along the ionic outer-sphere pathway for the high-valent oxorhenium(V) complex **1** catalyzed hydrolysis of trimethylsilane are shown in Figure 4 (black). This catalytic cycle can be divided into three steps: (1) the addition of silane to the metal center, **1**→**TS2**→**2cis**; (2) the heterolytic cleavage of Si–H bond upon the nucleophilic attack of water, **TS4anti**→**4anti**; (3) and the hydride transfer, **4syn**→**TS5**→**5**→ $\text{H}_2$  + silanol + **1**. Our calculated results indicate that the ionic outer-sphere pathway is thermodynamically favorable and is associated with a moderate activation free energy barrier (15.7 kcal/mol, **TS4anti**). Along the process of **TS4anti** → **4anti** → **4syn**, the free energy surface is considerably flat: **4syn** is 3.4 kcal/mol more stabilized than **4anti**. A negligible barrier is required for

hydride transfer (**TS5** relative to **4syn**). These results suggest that through the formation

Journal Name

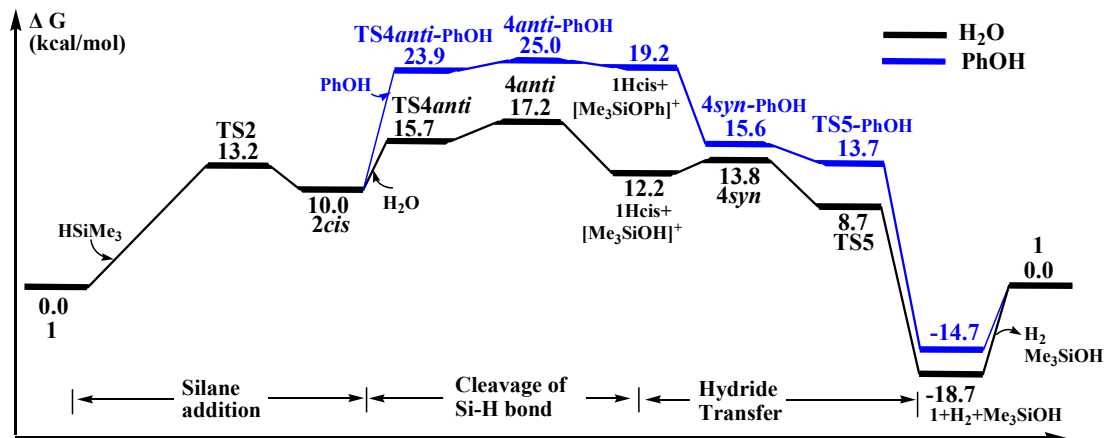


**Figure 4.** Schematic free-energy surface (B3LYP-D level) for the cationic high-valent oxorhenium complex  $[\text{Re}(\text{O})(\text{hoz})_2]^+$  (**1**) catalyzed the hydrolysis (black) and alcoholysis (blue) of silanes along the ionic outer-sphere mechanistic pathway.

of the ionic transition state **TS4anti** corresponding to the heterolytic cleavage of Si–H bond, isomerization within the intermediates of **4anti** and **4syn**, the hydride transfer process (**TS5**) readily occurs. This process may occur readily due to the strong electrostatic attraction between the hydride on the rhenium center and the solvated  $[\text{Me}_3\text{SiOH}_2]^+$  ion. The turnover-limiting step in the ionic outer-sphere pathway is related to the heterolytic cleavage of the Si–H bond (**TS4anti**). Overall, the calculated Gibbs energy barrier is close to the one experimentally reported (18.3 kcal/mol),<sup>31</sup> which supports the viability of the ionic outer-sphere mechanistic pathway. In addition, the large negative entropies found for this reaction<sup>31</sup> could be related with the intermolecular reaction disclosed by the ionic transition state **TS4anti**, which is a tighter arrangement and may imply large negative entropies. Furthermore, it is clear that along the ionic outer-sphere pathway, the generation of dihydrogen is comprised of one H atom from silane and one from water.

Abu-Omar *et al.* have shown that the cationic oxorhenium complex **1** is also effective for the highly efficient catalysis of alcohol silylation. Prompted by the above results, we have further explored the ionic outer-sphere free energy surfaces for **1**-catalyzed various alcohols ( $\text{CH}_3\text{OH}$ ,  $\text{EtOH}$ , and  $\text{PhOH}$ ) of silanes. Notably, the calculated rate-determining activation barriers of  $\text{CH}_3\text{OH}$  (15.4 kcal/mol) and  $\text{EtOH}$  (15.9 kcal/mol) are close to that of  $\text{H}_2\text{O}$  (15.7 kcal/mol). These values are consistent with the experimental observations that the silylation of primary alcohols are quite competitive with that of water. When moving to phenol ( $\text{PhOH}$ ), the substrate increases the barrier up to 25.0 kcal/mol kcal/mol (see Figure 4 (blue)), which indicates that phenol is not reactive. These results are also consistent with experimental observations. The optimized structure of the ionic transition state **TS4anti-PhOH** corresponding to heterolytic cleavage of Si–H bond upon the nucleophilic attack of phenol is shown in Figure 5. **TS4anti-PhOH** exhibits a late geometry in terms of short Re–H distance,  $d(\text{Re}-\text{H}) = 1.67 \text{ \AA}$  and long significant elongation of the Si–H bond,  $d(\text{Si}\cdots\text{H}) = 2.16 \text{ \AA}$ . The phenol is tightly coordinated to the silicon center, with a Si–O distance of 2.03 Å. Similarly, along the ionic mechanistic pathway of **TS4anti-PhOH** → **4anti-PhOH** → **4syn-PhOH**

(Figure 4 (blue)), the turnover-limiting step is also corresponding to the heterolytic cleavage of Si–H bond.

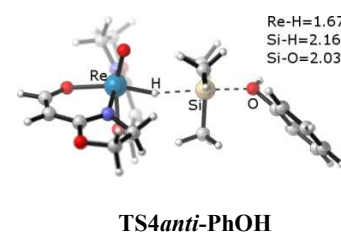


**Figure 5.** Optimized structure of the transition state **TS4anti-PhOH**, in oxorhenium(V) complex (**1**)-catalyzed the alcoholysis of phenol. Bond distances are shown in Å.

Moreover, our calculations indicated that the steric hindrance on silanes affect the catalytic reactivity of cationic oxorhenium(V) complexes (**1**) greatly.<sup>58</sup> By increasing the steric bulk of R substituents at the silicon atom, the reactivity of hydrosilanes catalyzed by the oxorhenium(V) complex **1**, are in order of decreasing activity:  $\text{EtMe}_2\text{SiH}$ ,  $\text{Et}_2\text{MeSiH}$ ,  $\text{Me}_3\text{SiH}$  (14.0, 14.8, and 15.7 kcal/mol) >  $\text{Et}_3\text{SiH}$  (16.5 kcal/mol) >  $t\text{BuMe}_2\text{SiH}$  (20.7 kcal/mol). The bulky  $t\text{BuMe}_2\text{SiH}$  increase the activation barrier largely to be 20.7 kcal/mol. Whereas, our results show that silanes bearing phenyl groups could reduce the activation barrier of the turnover-limiting steps. Reactions of water with  $\text{Ph}_2\text{MeSiH}$ ,  $\text{Ph}_3\text{SiH}$  (13.3 and 13.5 kcal/mol) proceeded at a slightly higher rates than  $\text{PhMe}_2\text{SiH}$  (15.2 kcal/mol), which indicated that the increase in activity of  $\text{Ph}_2\text{MeSiH}$  and  $\text{Ph}_3\text{SiH}$  compared to the less sterically hindered silane of  $\text{PhMe}_2\text{SiH}$ . This can be ascribed to stabilization of the solvated  $[\text{Me}_3\text{SiOHR}]^+$  ion by phenyl groups in the transition state structure. Therefore, these results indicated that a  $\text{S}_{\text{N}}2$  reactions is both affected by electronic effects between nucleophiles and substrates, as suggested in the nucleophilic substitution reaction at silicon ( $\text{S}_{\text{N}}2@(\text{Si})$ ) by Bickelhaupt.<sup>58</sup> In this regard, species with more nucleophilic character on the silicon group could play an important role in lowering the activation free energy.

## ARTICLE

Journal Name

**Pathway II: Oxorhenium(V) complex (1)-catalyzed hydrolysis/alcoholysis of silane via Cycle 1.** As described in the introduction, Abu-Omar *et al.* proposed a reaction pathway involving silane attacking a rhenium hydroxo complex (**1-OH**), resulting in a concurrent hydride transfer to yield silanol and a oxorhenium(V) hydride (Scheme 2, **Cycle 1**). However, as we tried to locate the transition state corresponding to abstraction of hydroxo group on **1-OH** by silane, all the attempts for searching such four-member ring of  $\sigma$ -bond metathesis-like transition state (**TS6trans** or **TS6cis**, shown in Scheme 5) failed. And we believed that even if such a transition state existed, it would definitely be higher.<sup>59</sup> Furthermore, the reaction to generate the rhenium hydroxo complex (**1-OH**) under the experimental environment was calculated to be highly endergonic,

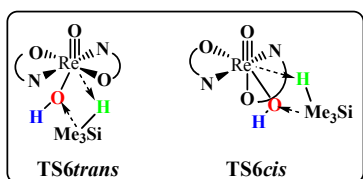


$\Delta G = 34.1$  kcal/mol (34.8 kcal/mol for **1-OHcis**). Hence, the low possibility of overcoming these high barriers when more competitive pathways (the ionic outer-sphere mechanistic pathway) indicates that **Cycle 1** does not contribute to the catalytic activity of oxorhenium(V) complex **1** catalyzed hydrolysis of silanes.

**Pathway III: Oxorhenium(V) complex (1)-catalyzed hydrolysis/alcoholysis of silanes via the oxidative addition pathway (Cycle 2).** Abu-Omar *et al.* has also suggested the possibility of the oxidative addition of Si–H bond to yield a transient rhenium(VII) complex. However, our theoretical calculations show that the rhenium(VII) species resulting from the oxidative addition of silane to the oxorhenium(V) complex **1** is not stable due to the crowd sphere. The structures of **TS7** and **7** (scheme 5, see Supporting Information for all the attempts) could not be found. Moreover, the oxorhenium(VII) intermediate resulting from the oxidative addition of Si–H bond to the rhenium complex isomer with dissociation of one oxazoline ring could not be located either (Scheme 5, **TS8-1** and **8-1**). Furthermore, the silane rhenium complex **8** with dissociation of one oxazoline ring is calculated not to be a feasible intermediate since it is placed at 44.8 kcal/mol above complex **1** and free silane. Therefore, our calculated results show that **Cycle 2** involving a transient rhenium(VII) complex is energetically unfavorable and can be ruled out as a likely mechanistic pathway.

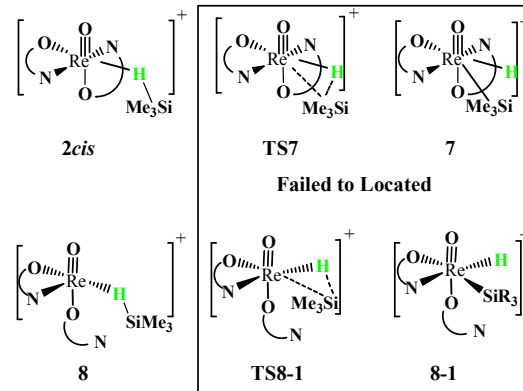
**Scheme 5** Other Si–H bond activation pathways.

**Attack of Si of the silane onto a rhenium hydroxo complex 1-OH**



**Failed to Located**

**Oxidative addition pathway**



## Conclusions

The mechanism of the high-valent cationic oxorhenium(V) complex  $[\text{Re}(\text{O})(\text{hoz})_2]^+$  (**1**) catalyzed hydrolysis and alcoholysis of organosilanes was extensively investigated using B3LYP-D level of theory. Remarkably, our computational results support that the ionic outer-sphere mechanistic pathway was the preferable route for the oxorhenium(V) complex (**1**)-catalyzed silane hydrolysis and alcoholysis. This mechanism involves the activation of Si–H through silane  $\eta^1$  bonding to the metal center and subsequent nucleophilic attack on  $\eta^1$ -silane via water or alcohol. Our calculations indicate that the rate-determining step is the nucleophilic *anti* attack at the silane center in the  $\eta^1$ -silane rhenium adduct **2cis**, which results in heterolytic cleavage of the Si–H bond. This transition structure (**TS4anti**) can be described as an  $\text{S}_{\text{N}}2$ -Si structure, with a silyl transfer to the oxygen of  $\text{H}_2\text{O}$  or alcohol and the concomitant formation of a neutral rhenium hydride. The heterolytic cleavage of the Si–H bond was calculated and associated with an activation free energy barrier of 15.7 kcal/mol for  $\text{H}_2\text{O}$ , close to that (18.3 kcal/mol) measurement with the experiments. During the ionic outer-sphere mechanistic catalytic cycle, a water/alcohol provides a hydride and together with a proton from the silane to generate  $\text{H}_2$ . It is the Lewis acidic metal center of the present catalytic system that renders the bound Si–H group more polarized in an adduct of silane rhenium complex; thus, the electrophilic character of the formed silane-rhenium complex is increased and it is much more susceptible to the nucleophilic attack by water or alcohol.

It is worth mentioning that the most important points that arose from our calculations are the that (1) the multiply bonded oxo ligand does not participate in the activation of the Si–H bond (**TS10**, 31.2 kcal/mol, Supporting Information), which is unlike the [2+2] addition mechanism, proposed by Toste and coworkers,<sup>60</sup> who suggest that the [2+2] Si–H bond addition across the metal oxo bond accounts for the carbonyl hydrosilylation reaction by the di-oxo-rhenium(V) complex  $\text{Re}(\text{O})_2\text{I}(\text{PPh}_3)_2$ , and (2) the high-valent oxorhenium(V) complex  $[\text{Re}(\text{O})(\text{hoz})_2]^+$  (**1**) is unique with regards to the catalytic hydrolysis and alcoholysis of organosilanes as it proceeds in an ionic outer-sphere manner. We demonstrated that the requirement of organic substrates coordination and insertion into the TM–H bond in ionic outer-sphere mechanisms is no longer necessary, which broadens the

## Journal Name

range of transition metals that can be used in such reactions. Finally, our calculations provide useful insight for the fundamental understanding of the activation of X–H bonds and the catalyzed reduction reactions mediated by high-valent oxo-metal complexes.

## Acknowledgements

We acknowledge the support of the National Natural Science Foundation of China (No. 21103093), the Jiangsu Province Science and Technology Natural Science Project (No. BK2011780), a Project Funded by the Priority Academic Program Development of Jiangsu Higher Education Institutions, and a Project Funded by Jiangsu Collaborative Innovation Center of Biomedical Functional Materials. We also thank the Shanghai Supercomputer Center and Nanjing University HPCC for their technical support.

## Notes and references

Jiangsu Collaborative Innovation Center of Biomedical Functional Materials, Jiangsu Provincial Key Laboratory for NSLSCS, College of Chemistry and Materials Science, Nanjing Normal University, Nanjing 210046, China email: weihaiyan@njnu.edu.cn

Electronic Supplementary Information (ESI) available: [Complete Ref. 45, comparison of different basis set levels, additional results not shown in the text, and Cartesian coordinates of all optimized structures discussed in the paper]. See DOI: 10.1039/b000000x/

- M. Jeon, J. Han and J. Park, *ACS Catal*, 2012, **2**, 1539.
- (a) J. F. Brown, *J. Am. Chem. Soc.*, 1965, **87**, 4317; (b) J. F. Brown and L. H. Vogt, *J. Am. Chem. Soc.*, 1965, **87**, 4313.
- R. Murugavel, A. Voigt, M. G. Walawalkar and H. W. Roesky, *Chem. Rev.*, 1996, **96**, 2205.
- G. Li, L. Wang, H. Ni and C. U. J. Pittman, *Inorg. Organomet. Polym.*, 2001, **11**, 123.
- E. W. Colvin, *Silicon Reagents in Organic Synthesis*; Academic Press: London, 1988; (b) S. E. Denmark and R. F. Sweis, In *Metal Catalyzed Cross-Coupling Reactions*; de Meijere, A., Diederich, F., Eds.; Wiley-VCH: Weinheim, 2004; Vol.1, chap. 4.
- S. T. Tan, J. W. Kee and W. Y. Fan, *Organometallics*, 2011, **30**, 4008;
- J. M. Brunel, *Int. J. Hydrog. Energy.*, 2010, **35**, 3401.
- W.-S. Han, T.-J. Kim, S.-K. Kim, Y. Kim, S.-W. Nam and S. O. Kang, *Int. J. Hydrog. Energy.*, 2011, **36**, 12305.
- (a) E. Lukevics and M. Dzintara, *J. Organomet. Chem.* 1985, **295**, 265; (b) D. Mukherjee, R. R. Thompson, A. Ellern and A. D. Sadow, *ACS Catal*, 2011, **1**, 698; (c) H. Mimoun, *J. Org. Chem.*, 1999, **64**, 2582; (d) Y. Ojima, K. Yamaguchi and N. Mizuno, *Adv. Synth. Catal.*, 2009, **351**, 1405; (e) M. Sridhar, J. Raveendra, B. C. Ramanaiah and C. Narsaiah, *Tetrahedron Lett*, 2011, **52**, 5980; (f) H. Ito, T. Saito, T. Miyahara, C. Zhong and M. Sawamura, *Organometallics*, 2009, **28**, 4829; (h) D. E. Barber, Z. Lu, T. Richardson and R. H. Crabtree, *Inorg. Chem.*, 1992, **31**, 4709; (i) M. J. Burn and R. G. Bergman, *J. Organomet. Chem.*, 1994, **472**, 43; (j) S. S. Yun, J. Lee, S. Lee and Kor. Bull, *J. Am. Chem. Soc.* 2011, **22**, 623.
- S. Wesley and P. Gerard, *J. Am. Chem. Soc.*, 2012, **134**, 17462.
- (a) For example, on the basis of the following bond energies [Me<sub>3</sub>Si-H (90.3 kcal/mol), Me<sub>3</sub>Si-OH (128 kcal/mol), H–H (104.2 kcal/mol), H–OH (116.0 kcal/mol), the hydrolysis of Me<sub>3</sub>SiH to give H<sub>2</sub> and Me<sub>3</sub>SiOH is exothermic by 26 kcal/mol; (b) R. Walsh, *Acc. Chem. Res.*, 1981, **14**, 246; (c) Darwent, B. deB. Nat. Stand. Ref. Data. Ser., Nat. Bur. Stand. (U.S.), 31 Jan 1970.
- E. Pouget, J. Tonnar, P. Lucas, P. Lacroix-Desmazes, F. Gannachaud and B. Boutevin, *Chem. Rev.*, 2010, **110**, 1233.
- For reference, the U.S. Department of Energy target for onboard hydrogen storage systems for light-duty vehicles was 4.5 wt % for 2010 and is 5.5 wt % for 2017. See: DOE Targets for Onboard Hydrogen Storage Systems for Light-Duty Vehicles, [http://www1.eere.energy.gov/hydrogenandfuelcells/storage/pdfs/targets\\_onboard\\_hydro\\_storage.pdf](http://www1.eere.energy.gov/hydrogenandfuelcells/storage/pdfs/targets_onboard_hydro_storage.pdf).
- (a) A. K. L. Teo and W. Y. Fan, *Chem. Commun.*, 2014; (b) S. C. Amendola, S. L. Sharp-Goldman, M. S. Janjua, N. C. Spencer, M. T. Kelly, P. J. Petillo and M. Binder, *Int. J. Hydrogen. Energy.*, 2000, **25**, 969.
- E. A. Ison, R. A. Corbin and M. M. Abu-Omar, *J. Am. Chem. Soc.*, 2005, **127**, 11938.
- (a) A. Weickgenannt, M. Mewald and M. Oestreich, *Org. Biomol. Chem.*, 2010, **8**, 1497; (b) R. J. P. Corriu and J. J. E. Moreau, *J. Chem. Soc., Chem. Commun.*, 1973, 38; (c) U. Oehmichen and H. Singer, *J. Organomet. Chem.*, 1983, **243**, 199; (d) B. T. Gregg and A. R. Cutler, *Organometallics*, 1994, **13**, 1039; (f) M. K. Chung and M. Schlaf, *J. Am. Chem. Soc.*, 2005, **127**, 18085; (h) T. Y. Lee, L. Dang, Z. Zhou, C. H. Yeung, Z. Lin and C. P. Lau, *Eur. J. Inorg. Chem.*, 2010, 5675; (i) A. Albright and R. E. Gawley, *Tetrahedron Lett*, 2011, **52**, 6130; (m) A. Krüger and M. Albrecht, *Chem. Eur. J.*, 2012, **18**, 652.
- M. Jeon, J. Han and J. Park, *ChemCatChem*, 2012, **4**, 521.
- G. H. Barnes, and N. E. Daughenbaugh, *J. Org. Chem.*, 1966, **31**, 885.
- J. John, E. Gravel, A. Hagège, H. Li, T. Gacoin and E. Doris, *Angew. Chem., Int. Ed.*, 2011, **50**, 7533.
- (a) K. Mori, M. Tano, T. Mizugaki, K. Ebitani and K. Kaneda, *New J. Chem.*, 2002, **26**, 1536; (b) T. Mitsudome, S. Arita, H. Mori, T. Mizugaki, K. Jitsukawa and K. Kaneda, *Angew. Chem., Int. Ed.*, 2008, **47**, 7938; (c) T. Mitsudome, A. Noujima, T. Mizugaki, K. Jitsukawa and K. Kaneda, *Chem. Commun.*, 2009, 5302.
- (a) E. Choi, C. Lee, Y. Na and S. Chang, *Org. Lett.*, 2002, **4**, 2369; (b) B. P. S. Chauhan, A. Sarkar, M. Chauhan and A. Roka, *Appl. Organomet. Chem.*, 2009, **23**, 385.
- (a) N. Asao, Y. Ishikawa, N. Hatakeyama, Y. Y. Menggenbateer, M. Chen, W. Zhang and A. Inoue, *Angew. Chem., Int. Ed.*, 2010, **49**, 10093; (c) L. Wanjun, W. Aiqin, Y. Xiaofeng, H. Yanqiang and Z. Tao, *Chem. Commun.*, 2012, **48**, 9183.
- Y. Mengmeng, J. Huize and F. Xuefeng, *Inorg. Chem.*, 2013, **52**, 10741.
- Y. Lee, D. Seomoon, S. Kim, H. Han, S. Chang and P. H. Lee, *J. Org. Chem.*, 2004, **69**, 1741; (b) X.-L. Luo and R. H. Crabtree, *J. Am. Chem. Soc.*, 1989, **111**, 2527; (c) L. D. Field, B. A. Messerle, M. Rehr, L. P. Soler and T. W. Hambley, *Organometallics*, 2003, **22**, 2387.
- (a) M. Lee, S. Ko and S. Chang, *J. Am. Chem. Soc.*, 2000, **122**, 12011.
- (a) M. R. Du-Bois and D. L. DuBois, *Chem. Soc. Rev.*, 2009, **38**, 62; (b) O. R. Luca, S. J. Konezny, J. D. Blakemore, D. M. Colosi, S. Saha, G. W. Brudvig, V. S. Batista and R. H. Crabtree, *New J. Chem.*, 2012, **36**, 1149; (c) A. L. Goff, V. Artero, B. Jousselme, P. D. Tran, N. Guillet, R. Métayé, A. Fihri, S. Palacin and M. Fontecave, *Science*, 2009, **326**, 1384.
- (a) J. L. Dempsey, B. S. Brunschwigg, J. R. Winkler and H. B. Gray, *Acc. Chem. Res.*, 2009, **42**, 1995; (b) V. Artero, M. Chavarot-*J. Name.*, 2012, **00**, 1-3 | 9

- Kerlidou and M. Fontecave, *Angew. Chem., Int. Ed.*, 2011, **50**, 7238; (c) Y. Sun, J. P. Bigi, N. A. Piro, M. L. Tang, J. R. Long and C. J. Chang, *J. Am. Chem. Soc.*, 2011, **133**, 9212; (d) B. D. Stubbart, J. C. Peters and H. B. Gray, *J. Am. Chem. Soc.*, 2011, **133**, 18070; (e) W. M. Singh, T. Baine, S. Kudo, S. Tian, X. A. N. Ma, H. Zhou, N. J. DeYonker, T. C. Pham, J. C. Bollinger, D. L. Baker, B. Yan, C. E. Webster and X. Zhao, *Angew. Chem., Int. Ed.*, 2012, **51**, 5941.
- 28(a) F. Gloaguen and T. B. Rauchfuss, *Chem. Soc. Rev.*, 2009, **38**, 100; (b) M. E. Carroll, B. E. Barton, T. B. Rauchfuss and P. J. Carroll, *J. Am. Chem. Soc.*, 2012, **134**, 18843; (c) T. Liu and M. Y. Darensbourg, *J. Am. Chem. Soc.*, 2007, **129**, 7008.
- 29 H. I. Karunadasa, E. Montalvo, Y. J. Sun, M. Majda, J. R. Long and C. J. Chang, *Science*, 2012, **335**, 698.
- 30 A. M. Appel, D. L. DuBois and M. R. DuBois, *J. Am. Chem. Soc.*, 2005, **127**, 12717.
- 31 R. A. Corbin, E. A. Ison, M. M. Abu-Omar, *Dalton Trans*, 2009, 2850.
- 32 (a) A. J. Chalk and J. F. Harrod, *J. Am. Chem. Soc.*, 1965, **87**, 16; (b) I. Ojima, M. Nihonyanagi and Y. Nagai, *J. Chem. Soc., Chem. Commun.*, 1972, 938a; (c) I. Ojima, T. Fuchikami and M. Yatabe, *J. Organomet. Chem.*, 1984, **260**, 335; (d) I. Ojima, M. Nihonyanagi, T. Kogure, M. Kumagai, S. Horiuchi and K. Nakatsugawa, *J. Organomet. Chem.*, 1975, **94**, 449.
- 33 K. A. Nolin, J. R. Krumper, M. D. Pluth, R. G. Bergman and F. D. Toste, *J. Am. Chem. Soc.*, 2007, **129**, 14684.
- 34 L. W. Chung, H. G. Lee, Z. Lin and Y. D. Wu, *J. Org. Chem.*, 2006, **71**, 6000.
- 35 P. J. Costa, C. C. Romão, A. C. Fernandes, B. Royo, P. M. Reis and M. J. Calhorda, *Chem. Eur. J.*, 2007, **13**, 3934.
- 36 M. Drees and T. Strassner, *Inorg. Chem.*, 2007, **46**, 10850.
- 37 K. Valliant-Ssunders, E. Gunn, R. G. Shelton, D. A. Hrovat, B. W. Thatcher and M. J. Mayer, *Inorg. Chem.*, 2007, **46**, 5212.
- 38 R. G. Parr and W. Yang, *Density Functional Theory of Atoms and Molecules*; Oxford University Press: New York, 1989.
- 39 (a) T. Robert and M. Oestreich, *Angew. Chem., Int. Ed. Engl.*, 2013, **52**, 5216; (b) A. Simonneau and M. Oestreich, *Angew. Chem., Int. Ed. Engl.*, 2013 **52**, 11905; (c) R. M. Bullock and M. H. Voges, *J. Am. Chem. Soc.*, 2000, **122**, 12594; (d) M. H. Voges and R. M. Bullock, *Dalton Trans*, 2002, 759; (e) G. Hairong, I. Masanori, P. Matthew, J. R. Norton and Z. Guang, *J. Am. Chem. Soc.*, 2005, **127**, 7805; (f) T. Y. Corey, *Chem. Rev.*, 2011, **111**, 863. (g) G. E. Dobereiner, A. Nova, N. D. Schley, N. Hazari, S. J. Miller, O. Eisenstein and R. H. Crabtree, *J. Am. Chem. Soc.*, 2011, **133**, 7547.
- 40 (a) D. J. Parks, J. M. Blackwell and W. E. Piers, *J. Org. Chem.*, 2000, **65**, 3090; (b) D. J. Parks and W. E. Piers, *J. Am. Chem. Soc.*, 1996, **118**, 9440; (c) D. J. Parks, W. E. Piers, M. Parvez, R. Atencio and M. J. Zaworotko, *Organometallics*, 1998, **17**, 1369; (d) J. M. Blackwell, E. R. Sonmor, T. Scoccitti and W. E. Piers, *Org. Lett.*, 2000, **2**, 3921; (e) A. Berkefeld, W. E. Piers and M. Parvez, *J. Am. Chem. Soc.*, 2010, **132**, 10660; (f) Z. Xiaoxi and D. W. Stephan, *J. Am. Chem. Soc.*, 2011, **133**, 12448; (g) S. J. Geier and D. W. Stephan, *J. Am. Chem. Soc.*, 2009, **131**, 3476.
- 41 (a) S. Park and M. Brookhart, *Organometallics*, 2010, **29**, 6057; (b) W. H. Bernskoetter, S. K. Hanson, M. Brookhart, *J. Am. Chem. Soc.*, 2009, **131**, 8603; (c) S. Park and M. Brookhart, *J. Am. Chem. Soc.*, 2012, **134**, 640; (d) J. Yang, P. S. White and M. Brookhart, *J. Am. Chem. Soc.*, 2008, **130**, 17509; (e) M. Findlater, W. H. Bernskoetter and M. Brookhart, *J. Am. Chem. Soc.*, 2010, **132**, 4534; (f) S. Park and M. Brookhart, *Chem. Commun.*, 2011, **47**, 3643; (g) J. Yang and M. Brookhart, *Adv. Synth. Catal.*, 2009, **351**, 175; (h) J. Yang and M. Brookhart, *J. Am. Chem. Soc.*, 2007, **129**, 12656; (i) S. Park, D. Bezier and M. Brookhart, *J. Am. Chem. Soc.*, 2012, **134**, 11404; (j) D. Bezier, S. Park and M. Brookhart, *Org. Lett.*, 2013, **15**, 496.
- 42 (a) J. M. Blackwell, K. L. Foster, V. H. Beck and W. E. Piers, *J. Org. Chem.*, 1999, **64**, 4887; (b) S. N. Blackburn, R. N. Haszeldine, R. V. Parish and J. H. Setchfield, *J. Organomet. Chem.*, 1980, **192**, 329; (c) J. Dwyer, H. S. Hilal and R. V. Parish, *J. Organomet. Chem.*, 1982, **228**, 191; (d) W. Wenmin, G. Piao, W. Yiou and W. Haiyan, *Organometallics*, 2014, **33**, 847; (e) O. G. Shirobokov, L. G. Kuzmina and G. I. Nikonov, *J. Am. Chem. Soc.*, 2011, **113**, 6487.
- 43 (a) E. A. Ison, J. E. Cessarich, G. Du, P. E. Fanwick and M. M. Abu-Omar, *Inorg. Chem.*, 2006, **45**, 2385; (b) G. Du and M. M. Abu-Omar, *Organometallics*, 2006, **25**, 4920; (c) E. A. Ison, E. R. Trivedi, R. A. Corbin and M. M. Abu-Omar, *J. Am. Chem. Soc.*, 2005, **127**, 15374; (d) G. S. Owens, J. Aries and M. M. Abu-Omar, *Catal. Today.*, 2000, **55**, 317; (e) G. Du, P. E. Fanwick and M. M. Abu-Omar, *J. Am. Chem. Soc.*, 2007, **129**, 5180.
- 44 (a) R. Krishnan, J. S. Binkley, R. Seeger and J. A. Pople, *J. Chem. Phys.*, 1980, **72**, 650; (b) A. D. Becke, *J. Chem. Phys.*, 1993, **98**, 5648; (c) P. J. Stephens, F. J. Devlin and C. F. Chaobalowski, *J. Phys. Chem.*, 1994, **98**, 11623; (d) C. Lee, W. Yang and R. G. Parr, *Phys. Rev. B.*, 1988, **37**, 785; (e) B. Miehlich, A. Savin, H. Stoll and H. Preuss, *Chem. Phys. Lett.*, 1989, **157**, 200.
- 45 M. J. Frisch, et al. Gaussian 09, Revision A. 02; Gaussian, Inc. Wallingford, CT, 2009.
- 46 (a) P. J. Hay and W. R. Wadt, *J. Chem. Phys.*, 1985, **82**, 299; (b) W. R. Wadt and P. J. Hay, *J. Chem. Phys.*, 1985, **82**, 284.
- 47 (a) A. W. Ehlers, M. Böhme, S. Dapprich, A. Gobbi, A. Höllwarth, V. Jonas, K. F. Köhler, R. Stegmann and G. Frenking, *Chem. Phys. Lett.*, 1993, **208**, 111; (b) A. Höllwarth, M. Böhme, S. Dapprich, A. W. Ehlers, A. Gobbi, V. Jonas, K. F. Köhler, R. Stegmann, A. Veldkamp and G. Frenking, *Chem. Phys. Lett.*, 1993, **208**, 237.
- 48 A. V. Marenich, C. J. Cramer and D. G. Truhlar, *J. Chem. Phys. B.*, 2009, **113**, 6378.
- 49 (a) S. Grimme, *J. Comput. Chem.* **2006**, *27*, 1787. (b) I. H. Kryspin, S. Grimme, *Organometallics* **2009**, *28*, 1001. (c) S. Grimme *J. Chem. Phys.* **2006**, *124*, 034108.
- 50 Legault, C. Y. CYLview, 1.0b; Université de Sherbrooke, 2009; <http://www.cylview.org>.
- 51 (a) J. Yang, P. S. White, C. K. Schauer and M. Brookhart, *Angew. Chem., Int. Ed.*, 2008, **47**, 4141; (b) G. Piao, W. Wenmin, W. Yiou and W. Haiyan, *Organometallics*, 2013, **32**, 47.
- 52 (a) K. Y. Dorogov, A. V. Churakov, L. G. Kuzmina, J. A. K. Howard and G. I. Nikonov, *Eur. J. Inorg. Chem.*, 2004, 771; (b) G. I. Nikonov, *Eur. J. Inorg. Chem.*, 2000, 1917.
- 53 (a) G. I. Nikonov, *Adv. Organomet. Chem.*, 2005, **53**, 217; (b) R. N. Perutz and S. Sabo-Etienne, *Angew. Chem., Int. Ed.*, 2007, **46**, 2578; (c) The calculated Re...Si distance is 4.25 Å in adduct **2trans**, which is significantly greater than the sum of the covalent radii of Re (1.28 Å) and Si (1.11 Å). The Re–H–Si bond angle is slightly bent, 174.4°. These features suggests that the rhenium-silane adduct **2trans** as an end-on η<sup>1</sup>-H(Si) coordination mode of

## Journal Name

- the silane. In  $\eta^2$ -SiH complexes, the Re–Si distances remain relatively short. (d) Piao, G.; Wenmin, W.; Yiou, W.; Haiyan, W. *Organometallics*. **2013**, *32*, 47.
- 54 The isomer of silane rhenium complex **2cis** (associating with higher energy) is shown in the Supporting Information.
- 55 (a) M. P. Doyle, K. G. High, V. Bagheri, R. J. Pieters, P. J. Lewis and M. M. Pearson, *J. Org. Chem.*, 1991, **18**, 206; (c) S. Chang, E. Scharrer and M. Brookhart, *J. Mol. Catal. A: Chem.*, 1998, **130**, 107.
- 56 Including the dispersion effect, the energy of ion pair **4anti** was calculated to be 1.5 kcal/mol higher than that of TS4anti, shown in the Supporting Information.
- 57 Inclusion of the dispersion effect, **TS5** is 5.1 kcal/mol lower than intermediate **4syn**, shown in the Supporting Information.
- 58 A. P. Bento and F. M. Bickelhaupt. *J. Org. Chem.*, 2007, **72**, 2201.
- 59 To obtain such a transition state, we could take the *syn* ionic transition states (**TS3syn** or **TS4syn**) as the reference structure (here, a hydroxo group instead of water). From this point, the silane moiety needs to be pushed close to the rhenium center—this imposes huge steric crowding. Therefore, we believed that even if such a transition state existed (**TS7anti**, **TS7syn**), it would definitely be higher.
- 60 (a) J. J. Kennedy-Smith, K. A. Nolin, H. P. Gunterman and F. D. Toste, *J. Am. Chem. Soc.*, 2003, **125**, 4056; (b) K. A. Nolin, R. W. Ahn and F. D. Toste, *J. Am. Chem. Soc.*, 2005, **127**, 17168.

## ARTICLE

SYNOPSIS TOC (Word Style "SN\_Synopsis\_TOC").

The ionic outer-sphere mechanistic pathway, which is initiated by the formation of a *cis*  $\eta^1$ -silane Re(V) adduct followed by the nucleophilic *anti* attack by either water or alcohol to the silicon atom, features a  $S_N2$ -Si transition as the most favorable pathway for the high-valent oxorhenium(V) complex catalyzed hydrolysis/alcoholysis of organosilanes.

